

Depth of faulting on Mercury: Implications for heat flux and crustal and effective elastic thickness

F. Nimmo¹

Department of Earth Sciences, University College London, England, UK

T. R. Watters

Center for Earth and Planetary Studies, National Air and Space Museum, Smithsonian Institution, Washington, DC, USA

Received 15 October 2003; revised 3 December 2003; accepted 17 December 2003; published 20 January 2004.

[1] Topographic profiles across a lobate fault scarp on Mercury have been used to constrain the depth of faulting to 30–40 km. Here we use this depth to place constraints on the crustal thickness and heat flow into the base of the crust. With no crustal heat production, the mantle heat flux on Mercury at the time of scarp formation was 30–50 mWm⁻². However, higher crustal heat production rates allow significantly lower mantle heat fluxes. In all cases the mantle heat flux exceeds the likely radiogenic heat flux 4 Gyr ago; it is likely that secular cooling accounted for the remainder. Irrespective of crustal heat generation, a crustal thickness of ≤ 140 km is required to satisfy both the faulting observations and the requirement that the base of the crust does not melt. The effective elastic thickness of the lithosphere at the time of faulting is predicted to be 25–30 km. **INDEX TERMS:** 5418 Planetology: Solid Surface Planets: Heat flow; 5475 Planetology: Solid Surface Planets: Tectonics (8149); 6235 Planetology: Solar System Objects: Mercury; 8010 Structural Geology: Fractures and faults; 8159 Tectonophysics: Rheology—crust and lithosphere. **Citation:** Nimmo, F., and T. R. Watters (2004), Depth of faulting on Mercury: Implications for heat flux and crustal and effective elastic thickness, *Geophys. Res. Lett.*, 31, L02701, doi:10.1029/2003GL018847.

1. Introduction

[2] Less is known about Mercury than any of the other terrestrial planets. One of the few clues to the properties of its crust and mantle is the existence of lobate scarps, thrust faults which probably developed in response to planetary contraction [Strom *et al.*, 1975; Watters *et al.*, 1998]. Recently, Watters *et al.* [2002] used the faulting observations to estimate the heat flux and lithospheric rigidity on Mercury. In this paper similar estimates are made, taking into account the likely rheology and distribution of heat producing elements within Mercury's crust.

2. Observations

[3] Lobate scarps are common landforms found in the hemisphere imaged by Mariner 10 [Strom *et al.*, 1975]. These features exhibit clear evidence of offset and hori-

zontal shortening and have thus been interpreted to be the expression of surface breaking thrust faults [Strom *et al.*, 1975; Melosh and McKinnon, 1988; Watters *et al.*, 1998, 2001]. Of the 82 lobate scarps mapped on the imaged hemisphere (Watters, T. R. *et al.*, Thrust faults and the global contraction of mercury, submitted to *Geophys. Res. Lett.*, 2003), over 30 have lengths >150 km. If the scarps are the result of global contraction, they may reflect from <1 km [Watters *et al.*, 1998] up to 2 km [Strom *et al.*, 1975] of decrease in the planetary radius. This contraction probably occurred after the end of the heavy bombardment, at approximately 4 Gyr B.P. [Melosh and McKinnon, 1988].

[4] Elastic dislocation modelling of the largest of the known lobate scarps, Discovery Rupes, suggests the underlying thrust fault has a planar geometry and a depth of faulting of 30–40 km [Watters *et al.*, 2002]. The similar across-strike widths of the other large-scale lobate scarps to Discovery Rupes [Watters *et al.*, 2001] suggests that similar depths of faulting are occurring. It is this depth of faulting which will be used to constrain the thermal structure of Mercury's lithosphere.

3. Method

[5] Near the surface, lithospheric material is cold and will deform in a brittle fashion, while at greater depths and temperatures, the rock is likely to undergo ductile flow. If the lithosphere is being flexed, part of it may alternatively undergo elastic (recoverable) deformation. The relevant stresses are given by [Scholz, 2002; Watts, 2001]

$$\sigma_b = f\rho gz, \quad \sigma_d = \left(\frac{\dot{\epsilon}}{A}\right)^{\frac{1}{n}} g_s^{\frac{p}{n}} e^{Q/nRT(z)}, \quad \sigma_e = \frac{EK}{1-\nu^2} \left(\frac{d}{2} - z\right) \quad (1)$$

where σ_b , σ_d and σ_e are the brittle, ductile and elastic stresses, respectively. Here ρ is density, g is acceleration due to gravity, z is depth, f is a frictional coefficient, $\dot{\epsilon}$ is the strain rate, g_s is grain size, A , n , p and Q are material constants, $T(z)$ is the temperature, R is the gas constant, E is Young's modulus, K is the down-dip curvature of the lithosphere, ν is the Poisson's ratio and d is the mechanical boundary layer (MBL) thickness. The maximum depth of faulting is determined by the depth at which σ_d equals σ_b .

[6] This brittle-ductile transition (BDT) depth depends on the temperature structure of the lithosphere. Here a simple two-layer model is assumed, in which a crust containing uniformly-distributed heat producing elements overlies the

¹Currently at Department of Earth and Space Sciences, University of California, Los Angeles, California, USA.

mantle. The resulting temperature structure within the crust is given by

$$T(z) = T_s + \frac{F_b z}{k} + \frac{Hz}{2k} (2h - z) \quad (2)$$

where T_s is the surface temperature, F_b is the heat flux into the base of the crust, k is the thermal conductivity, H is the heat generation within the crust and h is the crustal thickness. The temperature gradient within the mantle is simply F_b/k .

[7] Given a particular temperature structure, if the MBL is being flexed then equations (1) and (2) may be used to obtain its effective elastic thickness T_e as a function of curvature [McNutt, 1984; Watts, 2001].

4. Parameters

[8] Many parameters on Mercury are poorly constrained. The thickness of the crust is highly uncertain, although geodetic and crustal relaxation arguments produce a range of 100–300 km [Anderson *et al.*, 1996] and <200 km [Nimmo, 2002], respectively. Similarly, the composition of the crust is unclear, although the similarity of the reflectance spectrum and radar characteristics to those of the lunar highlands suggest that the crust is predominantly plagioclase [Vilas, 1988; Sprague *et al.*, 1997; Harmon, 1997]. Here we will adopt a dry anorthite rheology for the crust [Rybacki and Dresen, 2000], and a dry olivine rheology for the mantle [Karato *et al.*, 1986], and discuss the effects of these assumptions below. For plausible strain rates and temperatures, anorthite will deform by dislocation creep (unless $g_s < 0.1$ mm) and olivine by diffusion creep. The grain size for the olivine is assumed to be 1 mm.

[9] The depth to the BDT depends on the frictional behaviour of rock. Laboratory experiments show that the dry friction coefficient f is approximately 0.65, independent of rock type [Scholz, 2002]. This value predicts a thrust fault dip angle of 28.5°, similar to that inferred [Watters *et al.*, 2002].

[10] If the crust on Mercury is truly analogous to the lunar highlands, then the crustal concentration of heat producing elements will be roughly 8 times estimates of bulk silicate Earth (BSE) or bulk Moon concentrations (see Lodders and Fegley [1998] for estimated concentrations). Alternatively, if the crust is more basaltic, the crustal concentration of heat producing elements is likely to be lower. In view of these uncertainties, two end-member values of H are adopted. The first ($H = 0.465 \mu\text{Wm}^{-3}$) is appropriate for lunar highland material at 4.2 Gyr B.P.; the second, ($H = 0.065 \mu\text{Wm}^{-3}$) is appropriate for undepleted mantle material at the same time. The heat flux into the base of the crust F_b is treated as a free parameter.

[11] The strain rate during Mercury's early history is unknown. Thermal evolution models suggest a radial contraction of around 5 km in the first 0.5 Gyr, giving $\dot{\epsilon} \sim 10^{-19} \text{ s}^{-1}$ [Schubert *et al.*, 1988]. A spin-down time of 1 Gyr from a presumed initial 20 hr rotation period gives a similar value [Melosh and McKinnon, 1988]. Other sources of stress, such as convection or impacts, are likely to have produced higher strain rates. We will assume a strain rate of

10^{-17} s^{-1} and show below that the uncertainties have only minor effects on the results.

[12] Given a particular temperature structure for the MBL, its effective elastic thickness T_e may be calculated if the curvature is known [Watts, 2001]. The curvature is given by d^2w/dx^2 (where w is the vertical deformation), and for flexural features it scales as l/L^2 , where l is the vertical amplitude and L is a characteristic horizontal lengthscale. Three of the largest lobate scarps on the imaged hemisphere have mean vertical amplitudes and widths of 1.2 km and 50 km, respectively, [Watters *et al.*, 2001]. Equating these values with l and L , respectively, gives an estimate of K of $5 \times 10^{-7} \text{ m}^{-1}$. We will assume that the base of the MBL is defined by the 1400 K isotherm. This is a higher temperature than that used by Breuer *et al.* [1993], to account for the dryness of the lithosphere on Mercury.

5. Results

[13] Figure 1 plots the variation in BDT depth as a function of crustal thickness h and the heat flux F_b into the base of the crust. As F_b increases, the BDT depth decreases because the thermal gradient becomes steeper. Because the crust contains heat producing elements, an increase in h also causes a reduction in BDT depth, for the same reason. Depending on the crustal thickness and temperature structure, the first BDT transition may occur either within the crust or within the mantle. Figure 1 shows the resulting discontinuity in BDT depth as a result of this crust-mantle transition.

[14] The shaded areas in Figure 1 show the BDT depth range of 30–40 km inferred from the lobate scarp studies (see above). Figure 1a assumes a low value of H , while Figure 1b assumes a higher value. The result of the increased crustal heat generation is to move the BDT everywhere to shallower depths. The range of temperatures at a BDT depth of 30–40 km is 830–930 K. Figure 1a shows that BDT depths of 30–40 km may be obtained with base heat fluxes in the range 30–50 mWm^{-2} . Figure 1b shows that when crustal heat production is large, the range of acceptable values of F_b increases to 0–45 mWm^{-2} but the crustal thickness cannot exceed 120 km.

[15] If other processes, such as convective entrainment or phase transitions, do not intervene, the thickness of the crust will be limited by the temperature at which it melts. At the pressures of interest, pure anorthite melts at about 1800 K [Deer *et al.*, 2001, p. 753]. At this temperature, other likely minerals (and indeed the mantle) will be partially molten, so 1800 K is very much an upper bound. The contours in Figure 1 are dashed where the temperature at the base of the crust exceeds 1800 K. The requirements of a 30–40 km BDT depth and an absence of crustal melting together constrain the crustal thickness to <120 km.

[16] Although Figure 1 was produced assuming that h , F_b and H are independent, in reality they are coupled. If more radiogenic elements are present in the crust, the mantle heat production rate will be reduced and F_b will be lower. Figure 1 also shows the mantle radiogenic heat flux after crustal extraction (dot-dashed line), assuming bulk silicate Earth (BSE) abundances at 0.4 Gyr after solar system formation. Secular cooling will increase the value of F_b ; the value of F_b will be reduced at later times or if Mercury is

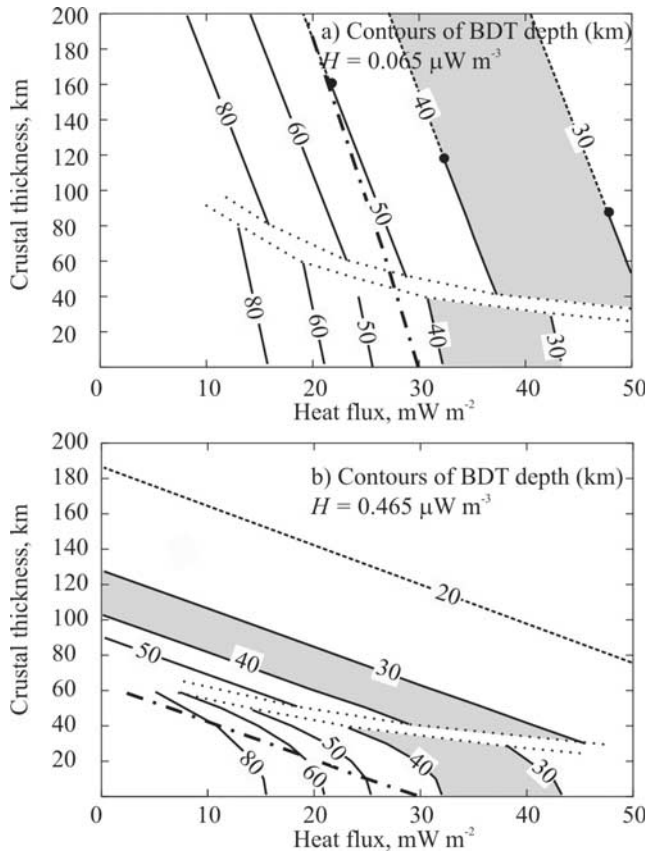


Figure 1. Depth to shallowest brittle-ductile transition (BDT) as a function of crustal thickness and heat flow into the base of the crust. Shaded regions indicate likely BDT depth based on observations of lobate scarps (see text). Black dots indicate the points at which the base of the crust reaches 1800 K; contours are dashed above this temperature. Dotted lines divide region where BDT occurs within mantle from region where BDT occurs within crust. Bold dashed-dotted line plots the radiogenic mantle heat flux after crustal extraction for bulk silicate Earth abundances at 0.4 Gyr after solar system formation. Strain rate is 10^{-17} s^{-1} ; other parameters are given in Table 1. a) Crustal heat generation rate $0.065 \mu\text{Wm}^{-3}$. b) Crustal heat generation rate $0.465 \mu\text{Wm}^{-3}$.

deficient in radiogenic elements compared with the Earth. The resulting lines plot to the left of the shaded areas, showing that an additional source of heat is required. The most likely source is secular cooling. Figure 1a shows that an extra 10 mWm^{-2} (equivalent to a mantle cooling rate of 167 K/Gyr) would be sufficient to shift the radiogenic heating line so that it plots in the shaded area.

[17] Given a particular temperature structure and curvature, the effective elastic thickness T_e may be calculated. Figure 2 plots T_e as a function of the brittle-ductile transition depth for two crustal thicknesses (20 km and 100 km) and the two heat generation rates used in Figure 1. Except for low values of F_b , when the MBL thickness becomes large, there is a consistent relationship between T_e and the BDT depth. For the curvature assumed here the ratio of T_e to BDT depth is about 0.75. Varying the curvature by an order of magnitude results in a ratio range of 0.35–1.5. The ratio is

not, however, particularly sensitive to the crustal thickness or heat generation rate.

6. Sensitivity Analysis

[18] In order to evaluate the effect of parameter uncertainties on the results, a model with a 40 km BDT depth and $T_e = 25 \text{ km}$ using $h = 60 \text{ km}$, $F_b = 36 \text{ mWm}^{-2}$ and $H = 0.065 \mu\text{Wm}^{-3}$ was adopted as a typical case. For this case an increase in BDT depth of 5 km corresponds to a reduction in heat flux of 4.5 mWm^{-2} .

[19] Changing the strain rate by \pm two orders of magnitude resulted in changes to the BDT depth of less than 10%. Using a diffusion creep plagioclase rheology ($g_s = 1 \text{ mm}$) resulted in a reduction in BDT depth of 5 km; with the same rheology but with a 10 mm grain-size the BDT depth increased by 3 km. Finally, using a dry diabase [Mackwell *et al.*, 1995] rheology resulted in a 6 km reduction in the BDT depth. It is thus apparent that the results shown in Figure 1 are rather insensitive to the exact rheology assumed. Because of the strong dependence of ductile creep on temperature, varying the slope of the frictional part of the curve by $\pm 20\%$ has only a small effect ($< 2\%$) on the BDT depth.

[20] The thermal structure of the crust has a strong influence on the BDT depth. For instance, increasing the surface temperature by 40 K reduces the BDT depth by 3 km. The $\sim 100 \text{ K}$ lateral variations in T_s across the planet [Soter and Ulrichs, 1967] might therefore be expected to have a significant effect on the spatial distribution and morphology of lobate scarps. Similarly, reducing the thermal conductivity k to $2.5 \text{ Wm}^{-1} \text{ K}^{-1}$ results in a reduction in BDT depth of 7 km if F_b stays constant. In practice, uncertainty about k will increase the uncertainty in F_b .

[21] An important constraint on the crustal thickness is that, as argued above, it must not exceed the melting temperature of anorthite (1800 K). This temperature is very much an upper bound; for more likely crustal solidus

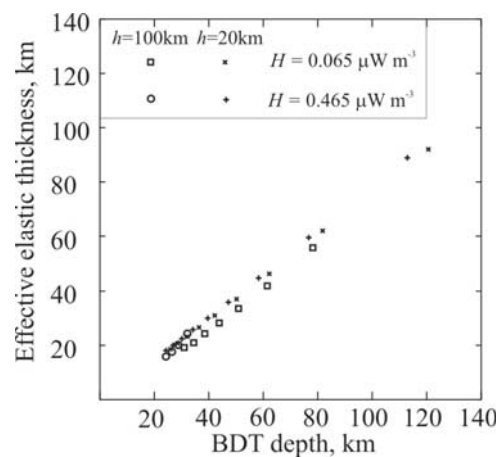


Figure 2. Predicted effective elastic thickness T_e and BDT depth as a function of crustal thickness h and crustal heat generation rate H for a curvature of $5 \times 10^{-7} \text{ m}^{-1}$. For each combination of h and H points were generated by increasing F_b in 5 mWm^{-2} increments from 10 mWm^{-2} (except for $h = 100 \text{ km}$, $H = 0.065 \mu\text{Wm}^{-3}$, which starts from $F_b = 15 \text{ mWm}^{-2}$).

Table 1. Parameters Used for the Nominal Model

Var.	Value	Units	Var.	Value	Units
g	3.76	m s^{-2}	T_s	400	K
ρ_c	2800	kg m^{-3}	ρ_m	3300	kg m^{-3}
f	0.65	-	$\dot{\epsilon}$	10^{-17}	s^{-1}
E	100	GPa	ν	0.25	-
k	3.0	$\text{W m}^{-1} \text{K}^{-1}$	K	5×10^{-7}	m^{-1}
n_c	3	-	n_m	1	-
A_c	5×10^{-6}	$\text{Pa}^{-3} \text{s}^{-1}$	A_m	7.7×10^{-14}	$\text{Pa}^{-1} \text{m}^2 \text{s}^{-1}$
Q_c	648	kJ mol^{-1}	Q_m	290	kJ mol^{-1}
p_c	0	-	p_m	2	-

The subscripts c and m refer to crustal and mantle values, respectively. Var. is variable.

temperatures of 1400–1600 K, the upper bound on crustal thickness in Figure 1a is reduced to 80–100 km.

[22] T_e is less sensitive than the BDT depth to variations in $\dot{\epsilon}$ or rheology. Varying the temperature at the base of the MBL by ± 200 K changes T_e by ± 3 km. Similar changes result for 20% variations in thermal conductivity. However, varying the curvature K has a large effect: a curvature of $5 \times 10^{-6} \text{ m}^{-1}$ results in $T_e = 12$ km while if $K = 5 \times 10^{-8} \text{ m}^{-1}$ then $T_e = 49$ km. Thus, by far the largest uncertainty in predictions of T_e are due to uncertainty in the curvature.

7. Discussion

[23] Figure 1 shows that the heat flux required to cause the observed BDT depths exceeds the likely radiogenic heat flux 4.2 Gyr ago. This is not a surprising result: Mercury was probably partially or totally molten at the end of its accretion [Schubert *et al.*, 1988], and will thus have cooled rapidly, generating a high initial heat flux.

[24] For a crust which is not highly enriched in heat producing elements (Figure 1a), the mantle heat flux was probably in the range 30–50 mWm^{-2} , similar to the range of 10–43 mWm^{-2} obtained by Watters *et al.* [2002]. However, for a more highly enriched crust, the heat flux range is 0–45 mWm^{-2} , a less useful constraint. It is thus only possible to place an upper bound on heat flux at the time the lobate scarps formed.

[25] On the other hand, Figure 1 shows that only crustal thicknesses ≤ 120 km are compatible with both the BDT depth and the requirement that the base of the crust not melt. Taking into account the likely uncertainties discussed above, a conservative upper bound on crustal thickness is 140 km. This constraint is compatible with estimates of $h < 200$ km based on viscous crustal relaxation [Nimmo, 2002], and the geodetic estimates of $h = 100$ –300 km [Anderson *et al.*, 1996].

7.1. Elastic Thickness Estimates

[26] Figure 2 shows that, for a scarp-like curvature, a BDT depth of 30–40 km implies a T_e of roughly 25–30 km, somewhat smaller than the ~ 40 km estimate obtained by Watters *et al.* [2002]. The T_e value thus obtained is relevant to the situation at the time the lobate scarps formed; on a cooling planet, the value of T_e at later times is likely to increase. Unless significant volcanic activity post-dated the formation of the scarps, or large spatial variations in T_e exist, the relatively low T_e values obtained here suggest that large uncompensated loads (mascons) are unlikely to exist.

[27] There are few other estimates of T_e on Mercury. Melosh [1977] argued that the observed global lineament distribution was consistent with tidal despinning when $T_e \leq 100$ km, a result compatible with those presented here. However, the style of faulting within the Caloris basin suggests an elastic thickness of 75–125 km at the time of smooth plains emplacement [Melosh and McKinnon, 1988]. Since the lobate scarps generally appear to postdate the smooth plains [Spudis and Guest, 1988], the discrepancy in T_e estimates is unlikely to be due simply to planetary cooling. One possible explanation is that the lithospheric curvature associated with Caloris is much smaller than that of the short-wavelength scarps, resulting in a higher rigidity for the same thermal structure [Watts, 2001, *c.f.*].

[28] An important result of this work is that the crustal thickness on Mercury is unlikely to exceed 140 km, or roughly 27% of the total mantle volume. For comparison, the ratios for the Moon, Mars and Venus are roughly 10%, 5% and 2%, respectively, and the mean lunar crustal thickness is about 60 km [Neumann *et al.*, 1996]. Both the crustal thickness and the elastic thickness estimates presented here will be tested when the forthcoming MESSENGER mission [Solomon *et al.*, 2001] returns high resolution gravity and topography data.

[29] **Acknowledgments.** This work was supported by the Royal Society and a grant from NASA's Planetary Geology and Geophysics Program.

References

- Anderson, J. D., R. F. Jurgens, E. L. Lau, M. A. Slade, and G. Schubert (1996), Shape and orientation of mercury from radar ranging data, *Icarus*, *124*, 690–697.
- Breuer, D., T. Spohn, and U. Wullner (1993), Mantle differentiation and the crustal dichotomy of Mars, *Planet Space Sci.*, *41*, 269–283.
- Deer, W. A., R. A. Howie, and J. Zussman (2001), *Rock-forming minerals vol. 4A: Framework silicates: Feldspars*, The Geological Society, London.
- Harmon, J. K. (1997), Mercury radar studies and lunar comparisons, *Adv. Space. Res.*, *19*, 1487–1496.
- Karato, S. I., M. S. Paterson, and J. D. Fitzgerald (1986), Rheology of synthetic olivine aggregates: Influence of grain-size and water, *J. Geophys. Res.*, *91*, 8151–8176.
- Lodders, K., and B. Fegley (1998), in *The Planetary Scientist's companion*, Oxford Univ. Press, New York.
- Mackwell, S. J., M. E. Zimmerman, D. L. Kohlstedt, and D. S. Scherber (1995), Experimental deformation of dry Columbia diabase: Implications for tectonics on venus, in *Rock Mechanics: Proceedings of the 35th US symposium*, edited by J. Daemen and R. Schultz, pp. 207–214, A. A., Balkema, Brookland, Vt.
- McNutt, M. K. (1984), Lithospheric flexure and thermal anomalies, *J. Geophys. Res.*, *89*, 11,180–11,194.
- Melosh, H. J. (1977), Global tectonics of a despun planet, *Icarus*, *31*, 221–243.
- Melosh, H. J., and W. B. McKinnon (1988), The tectonics of Mercury, in *Mercury*, edited by F. Vilas, C. Chapman, and M. Matthews, pp. 374–400, Univ. of Arizona Press, Tuscon.
- Neumann, G. A., M. T. Zuber, D. E. Smith, and F. G. Lemoine (1996), The lunar crust: Global structure and signature of major basins, *J. Geophys. Res.*, *101*(E7), 16,841–16,863.
- Nimmo, F. (2002), Constraining the crustal thickness on mercury from viscous topographic relaxation, *Geophys. Res. Lett.*, *29*(5), 1063, doi:10.1029/2001GL013883.
- Rybacki, E., and G. Dresen (2000), Dislocation and diffusion creep of synthetic anorthite aggregates, *J. Geophys. Res.*, *105*, 26,017–26,036.
- Scholz, C. H. (2002), *The mechanics of earthquakes and faulting*, Cambridge Univ. Press, Cambridge.
- Schubert, G., M. N. Ross, D. J. Stevenson, and T. Spohn (1988), Mercury's thermal history and the generation of its magnetic field, in *Mercury*, edited by F. Vilas, C. Chapman, and M. Matthews, pp. 429–460, Univ. of Arizona Press, Tuscon.
- Solomon, S. C., et al. (2001), The MESSENGER mission to Mercury: Scientific objectives and implementation, *Planet. Space. Sci.*, *49*, 1445–1465.

- Soter, S., and J. Ulrichs (1967), Rotation and heating of the planet Mercury, *Nature*, 214, 1315–1316.
- Sprague, A. L., D. B. Nash, F. C. Witteborn, and D. P. Cruikshank (1997), Mercury's feldspar connection mid-IR measurements suggest plagioclase, *Adv. Space Res.*, 19, 1507–1510.
- Spudis, P. D., and J. E. Guest (1988), Stratigraphy and geologic history of Mercury, in *Mercury*, edited by F. Vilas, C. Chapman, and M. Matthews, pp. 118–164, Univ. of Arizona Press, Tucson.
- Strom, R. G., N. J. Trask, and J. E. Guest (1975), Tectonism and volcanism on mercury, *J. Geophys. Res.*, 80, 2478–2507.
- Vilas, F. (1988), Surface composition of mercury from reflectance spectrophotometry, in *Mercury*, edited by F. Vilas, C. R. Chapman, and M. S. Matthews, pp. 59–76, Univ. of Arizona Press, Tucson.
- Watters, T. R., M. S. Robinson, and A. C. Cook (1998), Topography of lobate scarps on Mercury: New constraints on the planet's contraction, *Geology*, 26, 991–994.
- Watters, T. R., A. C. Cook, and M. S. Robinson (2001), Large-scale lobate scarps in the southern hemisphere of mercury, *Planet. Space Sci.*, 49, 1523–1530.
- Watters, T. R., R. A. Schultz, M. S. Robinson, and A. C. Cook (2002), The mechanical and thermal structure of Mercury's early lithosphere, *Geophys. Res. Lett.*, 29(11), 1542, doi:10.1029/2001GL014308.
- Watts, A. B. (2001), *Isostasy and flexure of the lithosphere*, Cambridge Univ. Press, Cambridge.
-
- F. Nimmo, Department of Earth Sciences, University College London, Gower St., London, WC1E 6BT, England, UK. (nimmo@ess.ucla.edu)
- T. R. Watters, Center for Earth and Planetary Studies, National Air and Space Museum, Smithsonian Institution, Washington, DC 20560, USA. (twatters@nasm.si.edu)